CHARACTERISTICS OF TURBULENCE SPECTRA IN DIFFERENT WEATHER PROCESSES UNDER UNSTABLE CONDITIONS*

Zhu Wenqin (朱文琴), *Zhu Cuijuan* (朱翠娟) and *Li Xingsheng* (李兴生)

Chinese Academy of Meteorological Sciences, Beijing 100081

Received November 20, 1993; revised April 25, 1994

ABSTRACT

In this paper, the data chosen from measurements by supersonic anemometers in Tongxian County of Beijing in 1990 are used to study characteristics of turbulence spectra in precipitation weather. Some turbulence parameters such as turbulence intensity, heat and momentum fluxes, friction velocity, M–O length and stability parameter are calculated and their dependence on turbulence spectra in different stability conditions are analyzed. Some encouraging results are obtained and compared with others' results.

Key words: turbulence spectra, wind velocity, stability, weather processes

I. INTRODUCTION

Turbulent flow, a kind of chaotic motion, prevails in the atmospheric boundary layer. Methods of mathematic statistics and spectral analysis are used to search for some regulations of turbulence. As a result, important principles of turbulence statistics theory have been found, and the relationship between correlation moments of some physical statistics and spectral density functions has been proved to be mutual Fourier transformation. Turbulence can be thought to consist of a series of eddies on different scales, and turbulence fluctuation energy can be expressed in terms of fluctuation frequencies or wavenumber. Studies of energy partition among various scales of eddies make us understand the fine construction of turbulence motion better.

Kaimal et al. (1972) analyzed turbulence spectra in the surface layer based on the Kansas experimental data and found that under different stability conditions subrange spectra on a log–log scale follows a power law of $-2/3$ in accordance with Kolmogorov's similarity theroy, but in the low frequency (LF) range, greater dispersion from the power law may be taken place (Kaimal 1978; 1988). Measurements with supersonic anemometers were made in Tongxian County, the east part of Beijing in 1990. Data selected for studies were under weather processes of shower or thunder shower. Analyses of turbulence characteristics and computation of energy spectra were made of the data chosen. Furthermore, diurnal variations of the above results and their relationships with stabilities were also studied. In addition, variations and differences in log–spectra of wind velocity were examined between convective weather and precipitation processes. Finally, our results were compared with some other researchers' work.

* This study is supported by the National Natural Science Foundation of China.

II. MEASUREMENT METHOD AND DATA PREPROCESSING

A time series of wind components and air temperature at a height of 30 m above the surface were obtained by supersonic anemometers at Meteorological Station of Tongxian County of Beijing in 1990. Measurements were taken at a rate of 10 s^{-1} with a sampling duration of 50—60 min every 3 hours. Sampling times were increased when there were weather processes. In order to decrease disturbances in sampling data, the raw data obtained were preprocessed as follows.

(1) *Outlier rejection*

Let $x(i)$ be the ith record in a time series $x(t)$, which has a mean value of $\bar{x}$ and the root mean square error S. If $x(i) > (\bar{x} + 5S)$ or $x(i) < (\bar{x} - 5S)$, then $x(i)$ can be considered as an outlier in the time series $x(t)$ because of its large deviation from $\bar{x}$. In this case, $x(i)$ as an outlier should be rejected from the time series $x(t)$, and may be replaced by a fixed $x'(i)$ defined as $x'(i) = [x(i-1) + x(i+1)] / 2$. Otherwise, $x(i)$ can be regarded as normal and retained in the data set to be analyzed.

(2) *Trend removal*

Trend in data is defined as any frequency whose period is longer than the record length. In the limit, the trend would be a linear one, say, $y = A_0 + A_1 t$, where y represents a physical quantity and is a function of t. Least square methods are often used to determine coefficients A_0 and A_1 in the trend equation.

If measurements are taken in an equal interval of time (Δt), the trend value for the ith record would be $y_i = A_0 + A_1 i \Delta t$. The raw data subtracting y_i would become the data set with trend removal.

(3) *Coordinate transformation*

In measurements the three axes (x, y, z) of a supersonic anemometer were taken eastward, northward and vertically upward, respectively. For the comparability of various results computed, a natural coordinate system is commonly chosen, taking the direction of horizontal prevailing wind as x axis, the direction of transverse wind as y axis, and the direction perpendicular to horizontal surface as z axis. For making this coordinate transformation, two mean components of the measured wind in a horizontal surface, $\bar{U}$ and $\bar{V}$ were first calculated, and then the azimuth α of horizontal prevailing wind against x axis was derived as $\alpha = \mathrm{tg}^{-1}(\bar{U} / \bar{V})$, ranging between 0 and 2π. Therefore, the data obtained in real measurements are able to transform to the corresponding components in the natural coordinate system, with a rotation of angle α.

III. CALCULATION OF QUANTITIES CHARACTERIZING TURBULENCE

According to Taylor's assumption, the fluctuation (f') of a physical quantity (f) such as u, v, w and t can be expressed as $f' = f - \bar{f}$, where $\bar{f}$ is the mean value of f. Advective transfer is related to $\bar{f}$, and turbulence transfer is related to f'.

Physical quantities characterizing turbulence such as fluctuation variance σ, turbulence intensity I, heat flux H, momentum flux M, friction velocity u_*, Monin–Obukhov (M–O) length L and stability parameter Z / L can be calculated from the following conventional expressions

(Kaimal et al. 1972; Li and Lu 1984; Lu and Li 1985):

$$\sigma = \sum_{i=1}^{N} \frac{(u_i - \overline{u})^2}{N}, \qquad (m^2\ s^{-2})$$

$$I = \frac{\sqrt{\sigma}}{\overline{u}}, \qquad \text{(dimentionless)}$$

$$H = \rho C_p \overline{w'T'}, \qquad (kcal\ m^{-2}\ s^{-1})$$

$$M = -\rho \overline{u'w'}, \qquad (kg\ m\ s^{-1})\ (m^{-2}\ s^{-1})$$

$$u_*^2 = (\overline{u'w'}^2 + \overline{v'w'}^2)^{1/2}, \qquad (m^2\ s^{-2})$$

$$L = -u_*^3 / \left(\kappa \frac{g}{\theta} \overline{w'\theta'}\right), \qquad (m)$$

$$\frac{Z}{L} = -\frac{(g/\theta)\overline{w'\theta'}}{u_*^3 / \kappa Z}, \qquad \text{(dimensionless)}$$

where u', v' and w' are fluctuating components of wind velocity in the longitudinal, transversal and vertical directions respectively. θ is the potential temperature; θ' the fluctuation of potential temperature; both of them can be replaced by their corresponding air temperatures, because the pressure at the height of sampling measurements is approximately 1000 hPa. κ is von Karman constant, taking 0.4, $g = 9.8$ m s^{-2}, ρ is air density, C_p is specific heat at constant pressure, and Z is the measurement height at 30 m.

Fast Fourier Transformation (FFT) can be employed to compute turbulence spectra whose high cut–off frequency is limited by sampling frequency, and low cut–off frequency is related to the length of data set (Huang and Li 1982). In order to lower the low cut–off frequency and expand the bandwidth of the spectra, the following treatment was made on our measurement data. The data every sampling interval (55—60 min) were in sequence divided into 8 segments, and each segment (about 7 min) included 4096 records. Then, turbulence spectra for each segment were calculated. Overlapping these spectra in terms of frequency and averaging them yielded the estimated spectra in the high–frequency (HF) range for one sampling time. On the other hand, a new data set was reconstructed by a 8–point moving average method from the raw data not to be segmented. This new data set has features of enlarged sampling interval and elongated data length. Spectral computation of the new data set gave the spectra in LF range. Finally, a spectrum curve with widened frequency range was thus obtained by the smooth conjunction of LF and HF range curves.

IV. RESULTS OF CALCULATION

The 15–min continuous data were taken for the calculation of quantities characterizing turbulence from which the data with wind velocity about 1 m s^{-1} were excluded because small wind velocity may cause large turbulence intensity (I) in calculation. The data chosen were on 24, 31 July and 1, 7 August 1990. In these days there were precipitation processes in daytime. It is seen from the results computed that I in daytime is stronger than that in nighttime. In general, I in the three directions of wind components reaches maxima in the afternoon. Enhancement in temperature and wind velocity makes I stronger. In overcast or rainy days, the diurnal variation in I has a small amplitude and I itself is also weak, due to small surface heating.

During period of thunder shower, increase in wind velocity makes I_u (longitudinal turbulence intensity) stronger. After raining, I_u, I_v and I_w are obviously weakened. The results computed also show that in fine days and the days of precipitation with slight variations in wind direction and velocity, there are relationships $I_u > I_v > I_w$. Figure 1 gives diurnal variations in I_u, I_v and I_w, on 24 July, which were the most obvious in diurnal variations of those days. It was a fine morning on 24 July, and a thunder shower occurred in about 1700—2000 BT (Beijing time) that day. Figure 1 shows that I_u, I_v and I_w are weakened starting from 1800 BT. During 0300—0600 BT, I_w has a decrease variation and reaches maximum at noon (1200 BT).

Other two parameters reflecting turbulence evolution are momentum and heat fluxes, which indicate the transfer capability of the momentum and heat across unit area in vertical direction in unit time, respectively. Positive heat flux means upward heat transfer, and conversely positive momentum flux means downward momentum transfer. Figure 2 depicts diurnal variations of heat flux in 3 days.

In general, heat flux is positive in daytime and negative in nighttime, but downward heat flux may exit even in daytime when there occurs thunder shower. Clearly shown in Fig.2 are the above phenomena that heat fluxes approach to zero or even negative at about 1630 BT 31 July and 1200 BT 7 August when it just was a raining period. In most cases, momentum fluxes are positive due to surface friction momentum-consuming.

It is clearly seen from our results computed that the stability parameter Z/L is commonly negative before thunder shower, and becomes near zero after it. There is a negative correlation between stability parameter and I_u, I_v or I_w, i. e. stability increasing against turbulence intensity decreasing.

It is known from M-O similarity theory that the dimensionless standard deviation of wind velocity ($\sqrt{\sigma}/u_*$) in the surface layer should tend to a constant. Listed in Table 1 are the dimensionless standard deviations of wind components: $A=\sqrt{\sigma_u}/u_*$, $B=\sqrt{\sigma_v}/u_*$ and $C=\sqrt{\sigma_w}/u_*$ calculated for $|Z/L|<0.2$.

The mean values for dimensionless standard deviations of wind components are $\bar{A}=2.51$,

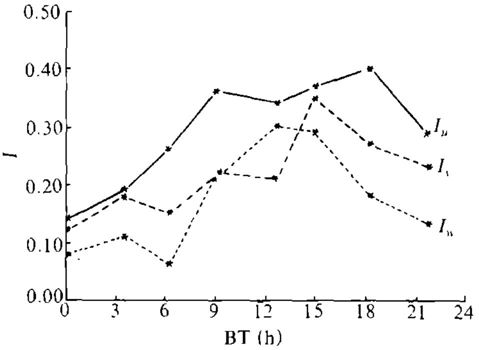

Fig. 1. Diurnal variations in turbulence intensity measured on 24 July 1990.

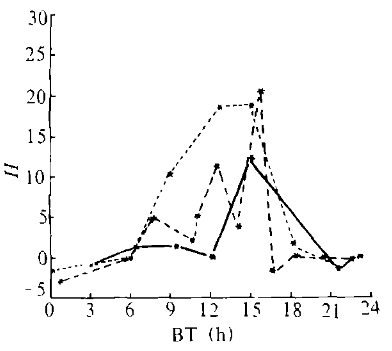

Fig. 2. Diurnal variations in heat flux on 24 July (dash), 31 July (longer dash) and 7 August (solid).

Table 1. Ratios (A, B, C) of Standard Deviation of Wind Components to Friction Velocity

Time	Z/L	$A=\sqrt{\sigma_u}/u_*$	$B=\sqrt{\sigma_v}/u_*$	$C=\sqrt{\sigma_w}/u_*$
2145 BT 24 July	0.0059	2.83	1.76	0.95
0300 BT 31 July	0.0450	2.16	1.64	1.36
1230 BT 31 July	0.0029	2.94	2.31	1.50
1635 BT 1 August	−0.019	2.43	1.37	1.09
1710 BT 1 August	−0.056	2.59	1.88	1.40
2200 BT 1 August	0.0420	2.42	2.10	1.35
1820 BT 7 August	0.0100	2.23	2.15	1.75
Mean		2.51	1.88	1.34

$\overline{B}=1.88$ and $\overline{C}=1.34$ respectively, which are comparable to $\overline{A}=2.39$, $\overline{B}=1.92$ and $\overline{C}=1.25$ obtained in flat areas by many researchers (see Zhao et al. 1991, p.84). All values of Z/L in Table 1 tend to zero which were calculated from the measurements after raining or during nighttime. This indicates that the neutral stratification often occurs after raining or in nighttime and in this time A, B and C tend to constants, which is in accordance with M—O similarity theory.

V. ANALYSES OF CHARACTERISTICS OF TURBULENCE SPECTRA

Wind velocity spectra were acquired by the smooth conjunction method mentioned in Section III. In this case the data length was taken to be one hour and sampling interval 0.1 s.

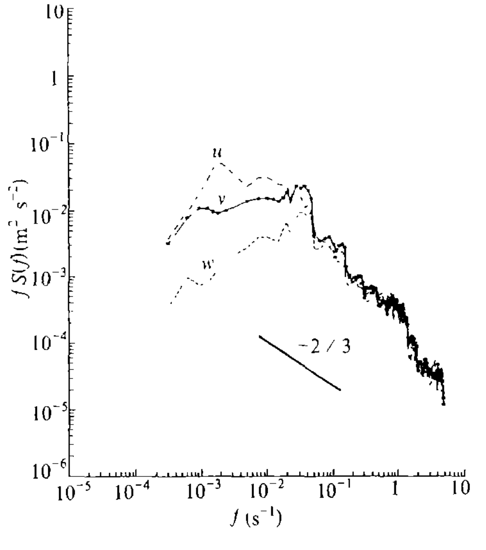

Fig. 3. Velocity spectra in 0700—0800 BT 7 August for $Z/L=-0.6$.

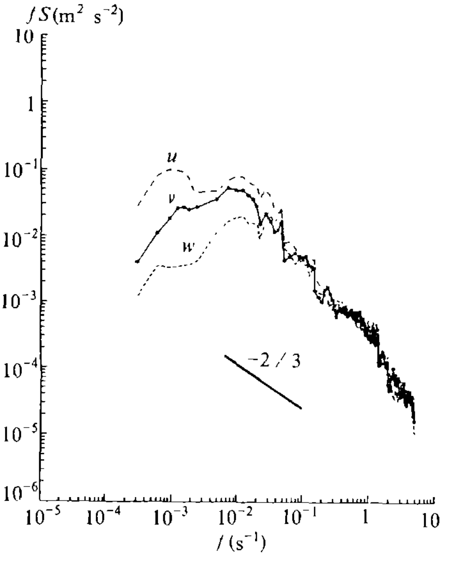

Fig. 4. Velocity spectra in 0900— 1000 BT 7 August for $Z/L=-5.6$.

Figures 3 and 4 delineate wind velocity spectra for negative values of Z/L in 0700—0800 BT and 0900—1000 BT 7 August, respectively. Negative Z/L indicates unstable conditions of the atmosphere. From these figures we can see that there exists such an obviously scatter sector from $f<0.02$ that $S_u(f)>S_v(f)>S_w(f)$. The results computed provide evidence that this kind of scatter sector always occurs in the weather of light rain or under neutral or stable conditions of the atmosphere after raining. If the length of sampling series is shorter, variations in wind velocity and direction are bigger, and the horizontal prevailing wind has an indefinite azimuth in the time period of sampling (i.e. prevailing wind has no longer prevailing sense), then the inequality $S_u(f)>S_v(f)$ does not hold any more. In HF range, three curves of $S_u(f)$, $S_v(f)$ and $S_w(f)$ approach to overlapping, and spectral density has an approximate relation of power $-2/3$ to frequency f. From Figs.3 and 4 we can see that in the range $0.05\ s^{-1}<f<1\ s^{-1}$ the overlapping curves conform well to the power law of $-2/3$. Under stable conditions, the range following the power law is wider because f can be extended to $0.01\ s^{-1}$. This tells us that stability influences the shape of spectral curve directly.

Let us examine the relation of velocity spectra with stability. Shown in Fig.5 are velocity spectra under different stabilities which were computed from the data on 31 July. Here only curves for vertical and longitudinal wind velocities are given, and curves for transverse wind velocity, which have similar forms, are not shown.

From Fig.5 it is seen that as Z/L increases, i. e. stability increases, spectral value decreases, and spectral curves in LF range are separated each other, with the curve corresponding to small Z/L above that to large Z/L. It is found that as instability increases, the energy–containing in LF range increases, which is affected evidently by stability. In HF range, when Z/L decreases from 1.12 to -0.017, the position of spectral curve lifts correspondently. We believe that when atmospheric conditions change from stable to unstable, energy–containing in LF range enhances. In the meantime, small eddies in HF range, through energy

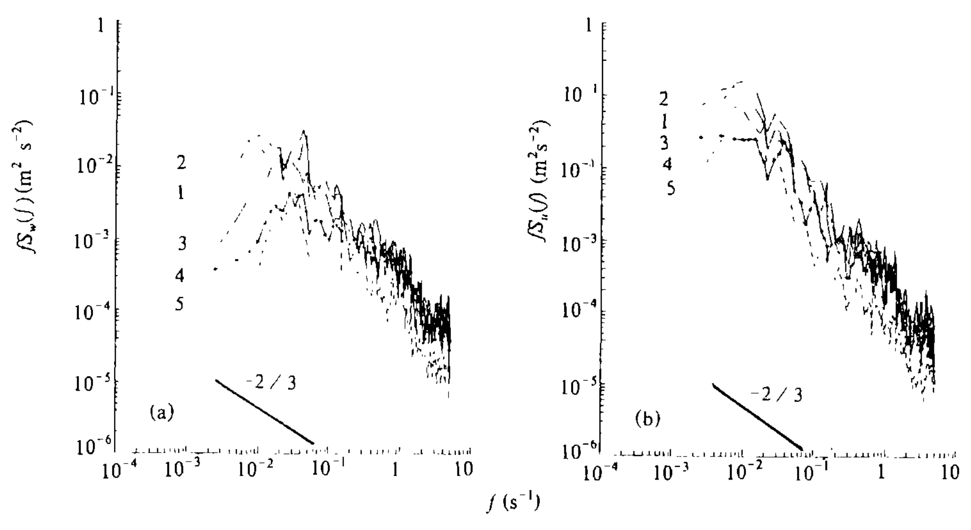

Fig. 5. Dependence of velocity spectra on stabilities for (a) vertical wind component and (b) longitudinal wind component. Curve 1 for $Z/L=-1.56$, 2 for -0.9, 3 for -0.017, 4 for 0.015 and 5 for 1.12.

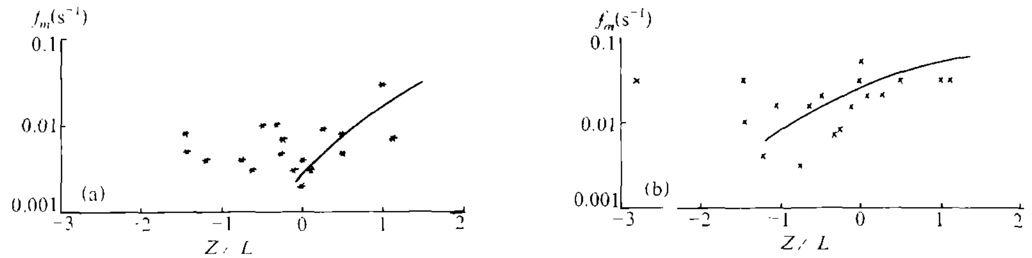

Fig. 6. Relationship of peak frequencies with Z/L for (a) longitudinal and (b) vertical wind component spectra.

cascade processes, gain and partly retain the energy from big eddies as energy sources, causing spectral curves to raise in position but the slope of curves remains unchange. However, in unstable conditions as Z/L continues to decrease, energy in LF range still changes but spectral curves in HF range tend to overlap, i.e. energy–containing in HF range does not increase any more, only playing a role of energy inertial transfer. It is seen from Fig.5 that the variation in amplitude of energy spectra is larger and more obvious in vertical wind component than in longitudinal one, because the data were chosen on the days when convective motion developed.

Figure 5a shows that peak frequencies in velocity spectra shift towards low frequencies as Z/L decreases, but this feature does not show obviously in Fig.5b. Delineated in Fig.6 are peak frequencies corresponding to more number of Z/L.

It is found from our results that the peak frequency of u spectra ranges between 0.002—0.01 s^{-1} (see Fig.6a), v spectra between 0.003—0.04 s^{-1} (figure not shown), and w spectra between 0.003—0.05 s^{-1} (see Fig.6b). Statistical mean of our results for unstable and neutral conditions leads to the following outcomes: $(f_m)_w = 0.02\ s^{-1}$, $(f_m)_u = 0.005\ s^{-1}$ and $(f_m)_v = 0.01\ s^{-1}$, where $(f_m)_w$, $(f_m)_u$ and $(f_m)_v$ denote peak frequencies in w, u and v spectra, respectively. The above results are in approximate agreement with relationships derived from Kansas data (see Zhao et al. 1991, p.108): $(f_m)_w = 5\,(f_m)_u = 2\,(f_m)_v$.

As Z/L decreases from 1 to 0, $(f_m)_u$ shifts towards LF evidently, and $(f_m)_w$ varies slightly because eddies in vertical direction may be restricted by the ground surface. However, as Z/L decreases from 0 to −1, $(f_m)_w$ shifts towards LF obviously but $(f_m)_u$ not, meaning that eddies in vertical direction develop fully with stability decreasing and convection developing greatly.

Take velocity spectra on 7 August as example. The three spectra in Fig.7 were derived from the data in 15 min length respectively starting at 1415 BT (light rain before thunder shower, $Z/L=-0.52$), at 1505 BT (thunder shower began, $Z/L=-0.17$), and at 1540 BT (it turned into light rain, $Z/L=-0.02$). In Fig.7 we can see that w spectra conform to the power law of $-2/3$ between frequencies 0.01— 1.0 s^{-1} (see Fig.7a), but u spectra decrease repidly after $(f_m)_u$ (see Fig.7b), leading to a narrower range which meets the power law of $-2/3$.

As stability becomes larger gradually, spectral density in LF range gets smaller and that in HF range first increases and then decreases. It is suggested that precipitation disturbs larger eddies, thus mean scales of turbulence get smaller, energy–containing in LF range decreases and spectral density in HF range increases with spectral peak shifting towards HF obviously. It is indicated from the above variation in spectra that turbulence motion in HF range is attributed to dynamic factors.

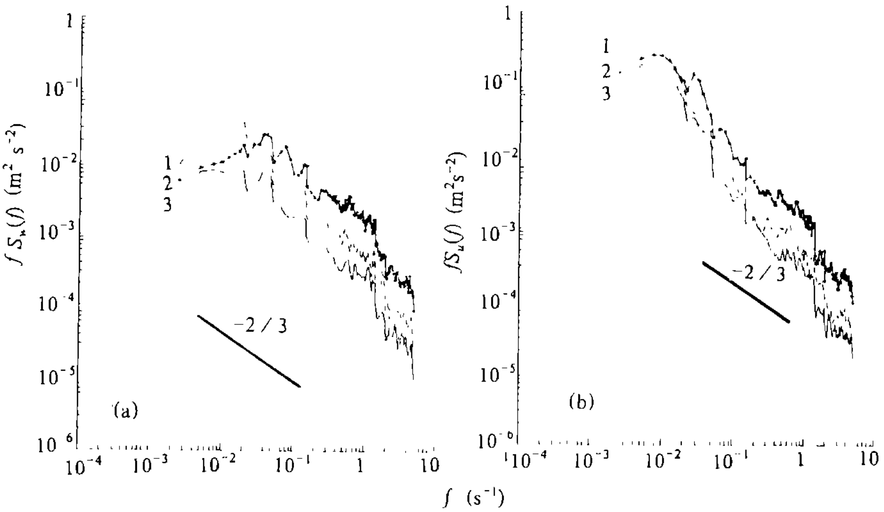

Fig. 7. Wind velocity spectra in the course of precipitation. (a) Vertical component spectra; (b) longitudinal component spectra. Curve 1 for $Z/L=-0.52$, 2 for -0.17 and 3 for -0.02.

VI. CONCLUSIONS

Through analysis and calculation of the data measured, the following conclusions can be drawn:

(1) Mean values of dimensionless standard deviation in u, v and w components in Tongxian County for Z/L vanishing are $A=2.51$, $B=1.88$ and $C=1.34$, which are in agreement with the results derived from flat areas by many foreign researchers.

(2) Transport of momentum and heat fluxes is influenced by turbulence intensity (I). In the daytime when I increases, heat flux is usually positive, meaning upward heat transport. After raining, however, air temperature decreases rapidly in surface layer, and negative heat flux occurs even in the daytime. As stability decreases, I increases, both of them have a good negative correlation.

(3) Negative Z/L of stability occurs before thunder shower. Within 1—2 hours after shower Z/L holds a small value close to zero, indicating a neutral atmospheric stratification.

(4) As to turbulence spectra in stable and neutral atmospheric stratifications in the surface layer of Tongxian County, its velocity spectra in HF range conform to the power law of $-2/3$ but in unstable conditions or in the course of thunder shower the above HF range becomes norrower.

(5) Velocity spectra in u, v and w scatter in LF range and tend to overlap in HF range. Stability mainly affects the scatter degree of spectra in LF range. As stability decreases, $(f_m)_w$, $(f_m)_u$ and $(f_m)_v$ all have a tendency to shift to LF.

(6) Larger eddies are easily disturbed by precipitation processes and mean scales of eddies get smaller. As a result, precipitation makes spectral density in LF range decrease all the time, but spectral density in HF range first increases and then decreases obviously with the end of precipitation. From the above variation it is seen that the turbulence motion in HF range is

attributed to dynamic factors.

REFERENCES

Huang Jiayou and Li Huang (1982), *Spectrum Analysis in Meteorology*, China Meteor. Press, Beijing, 318pp. (in Chinese).

Kaimal, J. C. (1978), Horizontal velocity in an unstable surface layer, *J. Atmos. Sci.*, **35:** 18—23.

Kaimal, J. C. (1988), *The Atmospheric Boundary Layer——Its Structure and Measurement*, Lecture Notes.

Kaimal, J. C., Wyngaarde, J. C., Izumi, Y. and Cote, O. R. (1972), Spectral characteristics of surface layer turbulence, *Quart. J. Roy. Meteor. Soc.*, **98:** 563—589.

Li Xingsheng and Lu Naiping (1984), Comparison of some computation methods for turbulence energy and flux, *Sci. Atmos. Sin.*, **8:** 315—321 (in Chinese).

Lu Naiping and Li Xingsheng (1985), Characteristics in wind direction fluctuation in the stable atmospheric boundary layer, *Acta Meteor. Sin.*, **43:** 35—44(in Chinese).

Zhao Ming et al. (1991), *Textbook on Boundary Layer Meteorology*, China Meteor. Press, Beijing, 466pp. (in Chinese).